Available online at www.sciencedirect.com
SCIENCE DIRECT
Applied Catalysis A: General 286 (2005) 85–95
APPLIED CATALYSIS A: GENERAL
www.elsevier.com/locate/apcata

Structural and textural characteristics of Ce-containing mordenite and ZSM-5 solids and FT-IR spectroscopic investigation of the reactivity of NO gas adsorbed on them

T.M. Salama [a], M.M. Mohamed [b], I. Othman A [a], G.A. El-Shobaky [c,*]

[a] *Faculty of Science, Chemistry Department, Al-Azhar University, Nasser City, Cairo, Egypt*
[b] *Faculty of Science, Chemistry Department, Benha University, Benha, Egypt*
[c] *National Research Center, Department of Physical Chemistry, Dokki, 12622 Cairo, Egypt*

Received 23 October 2004; received in revised form 7 March 2005; accepted 7 March 2005
Available online 20 April 2005

Abstract

The in situ interaction of nitric oxide (NO) gas on the cerium framework-substituted ZSM-5 and mordenite zeolites was studied by FT-IR spectroscopy. Samples of ZSM-5 and mordnite-containing cerium (7.5 wt.% expressed as CeO_2) have been hydrothermally synthesized from starting gel upon which the introduction of cerium is being made during synthesis of zeolites. The morphological and textural characteristics of cerium-free and cerium-containing zeolites were studied using XRD, FT-IR in the T–O range, and N_2 adsorption at −196 °C. The results revealed that the insertion of cerium in both zeolites led to a decrease in their degree of crystallinity. Such a decrease was 36% for Ce-ZSM-5 while it was 18% for Ce-mordenite. The results indicated a significant decrease in nitrogen sorption capacity (BET) by 31% from 624 to 431 m^2/g and also a decrease of the micropore volume by 27.8% from 0.579 to 0.418 cm^3/g for Ce-ZSM-5. These results were found on the other extreme in case of Ce-mordenite. The presence of Ce did not affect the cell volume of ZSM-5 much, while it increased that of mordenite. Most of Ce^{IV} ions were embedded in the framework of mordenite, where they exposed as extra-framework CeO_2 and cerium silicate in ZSM-5. The in situ interaction of NO on Ce-zeolites was studied using an FT-IR quartz cell. The adsorption of NO gas led to the formation of a series of nitrosyl species: N_2O (2245 cm^{-1}), NO^+ (2160 cm^{-1}), NO (1910 cm^{-1}), N_2O_3 (1880, 1580 cm^{-1}), $(NO)_{2s,as}$ (1844, 1734–1720 cm^{-1}), NO_2 (1630 cm^{-1}) and ionic compounds were stable upon evacuation, i.e. *nitrato* and *nitrito* NO_x^- (x = 2–3) (1300–1500 cm^{-1}). Such nitrosyl complexes were favorably formed on Ce-ZSM-5 than on Ce-mordenite due to facilitated intervention of the cerium couple (Ce^{III}/Ce^{IV}) on the former than on the latter.

Keywords: Ce-mordenite; Ce-ZSM-5; FT-IR investigation; NO adsorption

1. Introduction

The applications of zeolitic microporous materials in a diversity of chemical reactions have resulted in the development of new creation molecular sieves with different structures. The chemical composition, structure and extra-framework cations of the zeolite significantly affect the molecular adsorption–interaction with the zeolitic active sites, thus strongly influencing the catalytic properties of the zeolitic material [1–3]. An approach to achieve this goal is the isomorphous substitution of Al or Si in the zeolite framework by other atoms to prepare modified zeolites having new physicochemical and catalytic properties, which becomes an important research subject in the field of zeolitic chemistry [4].

Noble metals such as Rh, Pt and Pd are used for the catalytic decomposition of toxic gases like NO, CO and SO_2 released into the atmosphere from industrial and automobile exhaust sources. With an increase in global air pollution, efforts are being made to obtain more effective catalytic materials such as transition metal oxides in zeolites [5,6]. Actually the interaction of d-block transition metals with NO often involves a d-electron and/or an empty d-orbital,

* Corresponding author. Tel.: +20 2 7494265; fax: +20 2 3370931.
E-mail address: elshobaky@yahoo.com (G.A. El-Shobaky).

0926-860X/$ – see front matter © 2005 Elsevier B.V. All rights reserved.
doi:10.1016/j.apcata.2005.03.008

which leads to the formation of metal nitrosyls [7]. This species is supposed to be susceptible to decomposition depending on the mode of d-transition metals for NO coordination.

Cerium oxide, which is one of the important components of automotive and industrial exhaust catalyst, is active for NO_x removal, oxidation of CO and hydrocarbons and hydrogenation as well acts as oxygen storage in the lattice of cerium oxide [8]. The surface area and the type of active sites/species, however, are important factors in deciding the catalytic activity of a material. Because of the limitations in the surface area of cerium oxide, a high surface cerium-containing catalytic material using cerium-exchanged zeolites has been developed [9,10]. Yet, a little has been published on the application of Ce-zeolites as selective catalysts for the reduction of NO_x compounds. This was attributed to difficulties arisen due to a possible loss in the degree of crystallinity of Ce-exchanged zeolites during the exchange process [9,10], decreasing the thermal stability of zeolite, and the probability of forming CeO_2 segregates appear as clusters after calcination [11,12]. Consequently, it was required to incorporate Ce into the framework of mordenite and ZSM-5 as a result of the isomorphous substitution of Al by Ce, which can be obtained from starting gel. Cerium cation is known to show redox properties (Ce^{III}/Ce^{IV}), that can possibly account for a distinguished NO oxidation capacity of Ce-zeolite at low temperatures. The interaction of molecular species with active metal sites is usually studied with nitric oxide probe molecule using the FT-IR technique. In the present paper, the adsorption–interaction of NO with the active cerium species in the ZSM-5 and mordenite catalysts was compared.

2. Experimental

2.1. Materials

The materials used were: silicic acid powder, sodium hydroxide pellets (AR 98%), aluminum sulfate [Merck, $Al_2(SO_4)_3{\cdot}16H_2O$], *o*-phenylendiamine (Merck), Cerium nitrate [$Ce(NO_3)_3{\cdot}6H_2O$ 98%] and commercial H_2SO_4.

Details concerning methods of preparation of mordenite, ZSM-5 and Ce-containing relevant zeolites have been given elsewhere [13]. The amount of encapsulated Ce in zeolitic substrates during their synthesis was 7.5 wt.% and expressed as CeO_2. The samples were referred to as CeM_{in} and Ce-ZSM-5_{in} for Ce in mordenite and Ce in ZSM-5, respectively.

2.2. Experimental techniques

The X-ray diffractograms of various zeolitic samples were measured by using a Philips diffractometer (type PW 3710). The patterns were run with Ni-filtered copper radiation ($\lambda = 1.5404$ Å) at 30 kV and 10 m A with a scanning speed of $2\theta = 2.5^\circ$ min^{-1}.

In situ FT-IR spectra of the samples were recorded with JASCO single beam FT-IR 5300 spectrometer with 50 co-added scans at 2 cm^{-1} resolution. The sample was pressed into a self-supporting wafer and mounted in a quartz infrared cell with CaF_2 windows. The cell was connected to a closed circulating pyrex system with a dead volume of 301 cm^3 that is capable of reducing pressure to 10^{-6} Torr. The vacuum system was equipped with a vacuum gauge by which the experiments were conducted when the vacuum leveled to 10^{-5} Torr. The infrared cell was equipped with an electric furnace and the sample temperature was adjusted by using the temperature controller connected to a thermocouple made of nickel chrome. The IR sample was prepared by pressing the catalyst powder grounded in an agate mortar to a wafer of ca. 30 mg cm^{2-}. All IR spectra were collected at room temperature and presented by subtraction from the corresponding background reference.

The IR spectral changes due to adsorption of NO on CeM and Ce-ZSM-5 samples in the region of 2500–1300 cm^{-1} were evaluated. As a typical experiment the sample was thermally treated at 300 °C for 3 h under a reduced pressure of 10^{-5} Torr prior to admitting NO (50 Torr) gas at room temperature.

The reduction of catalyst samples was carried out by heating the wafer in H_2 atmosphere (50 Torr) for 30 min at 500 °C. A liquid nitrogen trap was installed to prevent reoxidation of sample by evolved water. Following this, the system was evacuated for 15 min to remove gaseous hydrogen at the same temperature.

The nitrogen adsorption isotherms were measured at −196 °C using a conventional volumetric apparatus. The specific surface area was obtained using the BET method. The micropore volume and the external surface area were obtained from the *t*-plot method.

3. Results and discussion

3.1. XRD and surface properties

The X-ray diffractograms of pure zeolites, Ce-M_{in} and Ce-ZSM-5_{in} are shown in Fig. 1. XRD patterns did not confirm the presence of CeO_2 species in Ce-M_{in} but a little crystalline feature of this phase in Ce-ZSM-5_{in} at $2\theta = 25.850$, 39.480 and 42.440 are depicted, in addition to a broad line at $2\theta = 26.63$ characteristic of α-quartz (Si_3O_6) phase. Furthermore, both the diffractograms of zeolite samples include small diffraction peaks characteristic for cerium silicate [$Ce_2(Si_2O_7)$] [14]. It seems that cerium is well suited in CeM_{in} rather than in Ce-ZSM-5_{in}. The noticed decrease in crystallinity of zeolite samples following cerium incorporation could be due to a possible destruction of some frameworks during synthesis, due to the bulky size of cerium ions compared with that of Na ones.

The BET surface area of cerium-free mordenite (289 m^2/g) was lower than that of CeM_{in} (331 m^2 g^{-1}). Besides, the

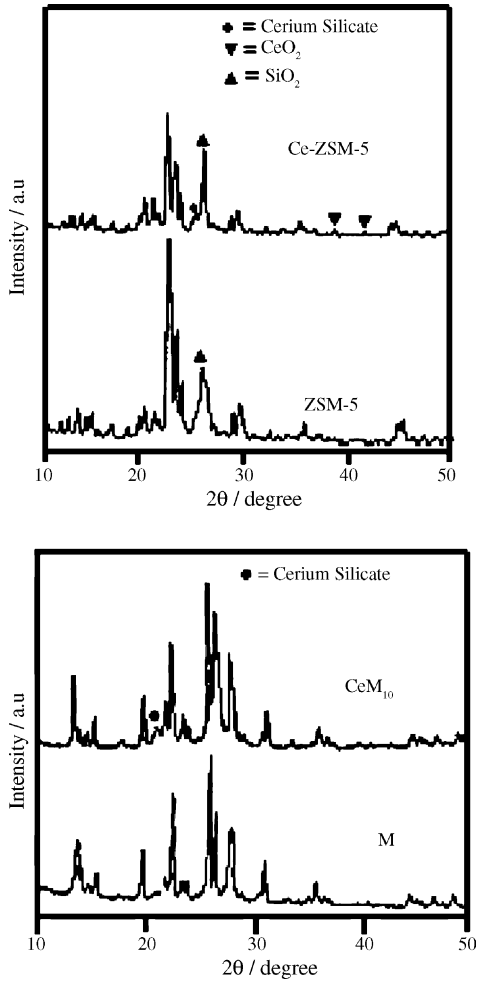

Fig. 1. X-ray powder diffraction patterns of synthesized zeolites and after incorporation with CeO_2.

total pore volume of the latter (0.322 cm^3/g) was higher than that of the former (0.285 cm^3/g) (Table 1), indicating the involvement of cerium in the framework of mordenite zeolite.

The V_{l-t} plot of CeM_{in}, at $p/p^0 = 0.35–0.85$, indicates an upward t deviation starting at 4.3 Å and extended up to 11.5 Å, whereas that of cerium-free mordenite showed an upward deviation starting at $t = 5.3$ Å (Fig. 2). This result demonstrates widening of the pores in the former sample compared with the latter one, together with the absence of pore blockage due to oxide formation as has been confirmed

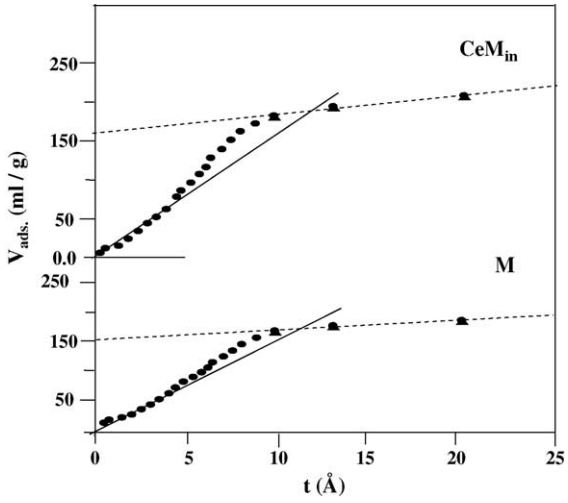

Fig. 2. V_{l-t} plots of synthetic mordenite sample and modified by CeO_2.

from XRD analysis. This result was confirmed from the increase in total pore volume (V_p) of wide pores (V_p^{wid}) from 0.0575 cm^3/g in mordenite to 0.0746 cm^3/g in CeM_{in}. The unit cell volume of CeM_{in} was found to be higher than that of mordenite reflecting the well incorporation of cerium in the framework of mordenite (Table 1).

On the other hand, the BET surface area of Ce-ZSM-5_{in} (431 $m^2\ g^{-1}$) was lower than that of cerium-free ZSM-5 (624 m^2/g) (Table 1), implying blocking of some pores of ZSM-5 with CeO_2 and $Ce_2(SiO_7)$ species. The revealed decrease of V_p in Ce-ZSM-5_{in} (0.418 cm^3/g) compared with that in ZSM-5 (0.579 cm^3/g) supports the latter suggestion. Indeed, the unite cell volume was found to be lower in Ce-ZSM-5_{in} than that in ZSM-5 (Table 1), signifying the presence of CeO_2 and/or cerium silicate species inside the ZSM-5 channels. In addition, the V_{l-t} plot of the Ce-ZSM-5_{in} sample (Fig. 3) showed a non-defined upward deviation followed by an earlier downward deviation at $t = 8$ Å if compared with that of CeM_{in}, giving a clue about the pore blockage in Ce-ZSM-5_{in}.

3.2. Framework structure

Infrared spectra of the zeolite lattice vibrational modes observed between 450 and 1300 cm^{-1} were recorded for the different samples (Fig. 4). As it can be seen, the bands associated with the structural tetrahedra in mordenite,

Table 1
Surface characteristics, unit cell parameters and degree of crystallinity of different zeolite samples investigated

C[a] (%)	V (Å)^3	Cell parameters (Å)			Microporosity (%)	r (Å)	V_p^{wid} (cm^3/g)	V_p^{μ} (cm^3/g)	V_p^{total} (cm^3/g)	S^{wid} (m^2/g)	S^{ext} (m^2/g)	S^{μ} (m^2/g)	S_{BET} (m^2/g)	Samples
		c	b	a										
100	2797	7.536	2797	18.022	94	25	0.0575	0.268	0.285	64	30	307	289	Mordenite
78	2946	7.661	2947	18.838	77	24	0.0746	0.247	0.322	77	38	254	331	Ce-mordenite
100	5350	13.413	5350	19.041	83	23	0.0973	0.481	0.579	105	50	519	624	ZSM-5
64	5322	13.364	5322	19.8522	85	24	0.0634	0.354	0.418	66	30	365	431	Ce-ZSM-5

[a] The values of C given in this column refer to the degree of crystallinity of zeolite samples investigated and considered as 100% for the cerium-free samples. The peak height of the main diffraction line of zeolite sample was considered as a measure of its degree of crystallinity.

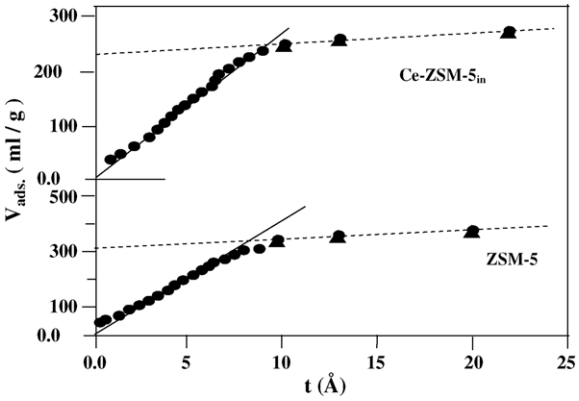

Fig. 3. V_{l-t} plots of synthetic ZSM-5 sample and modified by CeO_2.

namely T–O in five-membered rings (582 cm^{-1}), and Al–O vibrations belonging to alternate SiO_4 and AlO_4 tetrahedra and/or single four-membered rings (629–640 cm^{-1}) [15] are retained in CeM_{in} which reflects the intact structure of the zeolite framework following Ce incorporation. The absorption band at 720 cm^{-1} in the spectrum of CeM_{in} due to isolated AlO_4 tetrahedra in four-membered rings was shifted downward to 693 cm^{-1}. However, the coexistence of a broad band at 800 cm^{-1} due to symmetric T–O stretching vibration of the aluminosilicate lattice in M and CeM_{in} indicates that dealumination of the mordenite lattice after inclusion of Ce must be excluded. Such dealumination requires, in contrast, upward shift of this band to higher frequencies as well as an increase in its intensity [16]. However, the devoted increase in wavenumber of the T–O asymmetric stretching vibration at 1078 in M to 1089 cm^{-1} in CeM_{in} was due to substitution of Al by Ce that was intentionally performed during the synthesis process.

The spectrum of Ce-ZSM-5_{in} showed some variations from that of cerium-free ZSM-5, in the sense that ν_{as}T–O at 1088(1092) cm^{-1} was markedly decreased in intensity together with the one at 1224 cm^{-1} assigned to the same mode vibration after cerium incorporation. This indicates that some deformation of aluminosilicate lattice is demonstrated for this sample. Such deformation did not occur in CeM_{in} plausibly due to the larger pore windows devoted for the mordenite structure that accommodate Ce atoms. The small bands simultaneously delivered at 694 and 622 cm^{-1} in the spectrum of Ce-ZSM-5_{in} are most likely due to cerium silicate species. This observation is associated with the increase in the absorption at 796 cm^{-1} thus exposing more unshielded Al–O bonds to vibrate in the T–O linkages. These consequences are confirmed by the observed lower value of micropore volume of Ce-ZSM-5_{in} than that of Na-ZSM-5, implying the presence of some amorphous structures inside ZSM-5 channels.

3.3. Adsorption of NO on Na-ZSM-5

Fig. 5 shows the in-situ FT-IR spectra of NO adsorbed at room temperature on Na-ZSM-5 (dehydrated at 300 °C) in

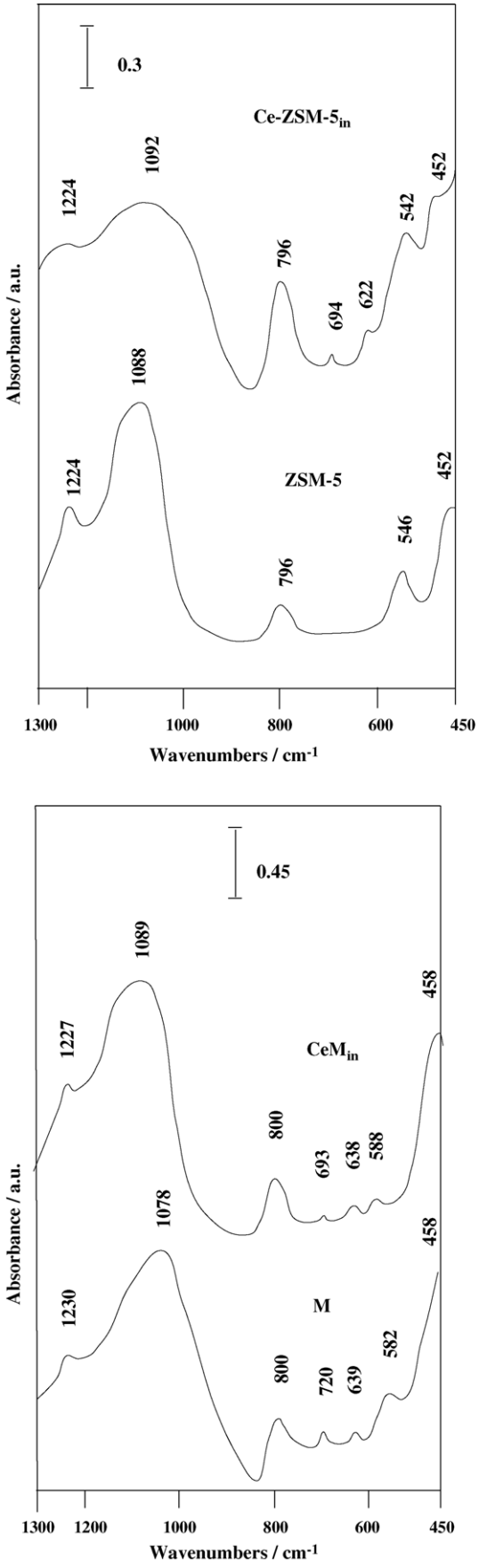

Fig. 4. FT-IR spectra of zeolites and Ce/zeolites samples.

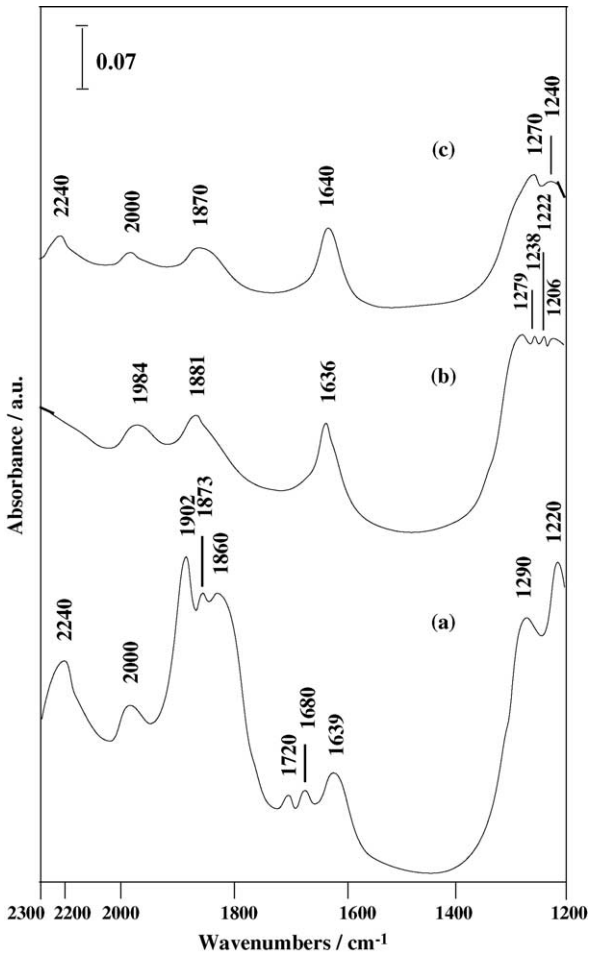

Fig. 5. FT-IR spectra of NO adsorbed on Na-ZSM-5 at room temperature: (a) in the presence of NO gas phase (50 Torr), (b) after (a) evacuation at room temperature and (c) evacuation at 50° following NO (50 Torr) adsorption at room temperature.

equilibrium with 50 Torr of NO at room temperature, after evacuation at room temperature and at 50 °C. The adsorption of NO showed intense bands at 1902, 1873 and 1860 cm^{-1}, moderate intense ones at 1720, 1680 and 1639 cm^{-1} in addition to small bands at 2240 and 2000 cm^{-1}. In the 1300–1200 cm^{-1} region, bands at 1290 and 1220 cm^{-1} appeared as well. The spectral features at 1873 and 1860 cm^{-1} are due to ν(N–O) symmetric in $(NO)_2$, and that at 1720 and 1680 cm^{-1} to ν(N–O) asymmetric vibration of the same species, in conformity with those identified by Yoshinobu and Kawai (1865, 1859 cm^{-1}) of NO adsorption on aluminum oxide supported palladium [17]. The 1902 cm^{-1} band has been observed by many authors for NO_x sorption and has been attributed to N–O vibration in NO bound to coordinatively unsaturated site (cus) [18]. The band at 2240 cm^{-1} is attributed to the stretching vibration of N–N in N_2O species inconsistent with the assignment made for the same species on NaY zeolite (2240 cm^{-1}) [19,20]. The occurrence of N_2O species is ascertained by the band at 1290(1220) cm^{-1} that assigned to ν(N–O) species in N_2O in conformity with that depicted previously on NaY [21]. The absorption band at 1639 cm^{-1} can be assigned to adsorbed NO_2 species [21].

Upon evacuation of the system at room temperature, reversibly attached species at 2240 cm^{-1} disappeared together with those at 1902, 1860, 1720 and 1680 cm^{-1} leaving less intense bands at 1984, 1881 and 1636 cm^{-1}. Warming up the temperature to 50 °C decreased the NO_2 (1640 cm^{-1}) band with the bands occurring at 1881(1870 cm^{-1}) of adsorbed dinitrosyls $(NO)_2$. The bands at 2240 and 1270 cm^{-1} of chemisorbed N_2O species on ZSM-5 surface were simultaneously delivered. The presence of N_2O species at 50 °C was a result of NO disproportionation. Thus, it can be concluded that NO reacts to form $(NO)_2$, N_2O and NO_2 adsorbed species on ZSM-5.

3.4. NO adsorption on Ce-ZSM-5_{in}

Fig. 6 shows the IR spectra of the NO adsorption (50 Torr equilibrium pressure) at room temperature on dehydrated Ce-ZSM-5_{in} (300 °C, 3 h). The spectra monitored after gas admission, evacuation at room temperature and 50 °C. Small bands produced at 2240 and 2225 cm^{-1}, which appeared parallel to those at 1287 and 1225 cm^{-1} are attributed to N_2O species. The medium band at 1877 cm^{-1} and a small hump at 1580 cm^{-1} are caused by adsorbed N_2O_3 species, and the band at 1645 cm^{-1} assigned to Ce^{4+}-NO_2. These assignments are in good agreement with those published previously [22,23]. The small bands at 1580, 1520 and 1491 cm^{-1} are locating in the region of typical bi- and monodentate nitrato (NO_3^-) species [24,25].

The presence of N_2O and NO_3^- suggests a disproportionation of NO with the formation of adsorbed NO_2 (1645 cm^{-1}) species. Disproportionation of NO was reported over a variety of metal ions in zeolites, e.g. Cu-ZSM-5 [26] and Au-Y [27] at room temperature. The observed activity may be accounted for the enhanced polarization due to electrostatic potential associated with the presence of metal cations with a high valence state in zeolite, i.e. Ce^{n+} (n = 3–4) [28]. In addition, metal ions could also offer adsorption sites for NO, for instance in the form of an oxygen-coordinated hyponitrite ion $(N_2O_2)^{2-}$, which is subject to decomposition into N_2O over CeO_2 [29]. An alternative explanation for the presence of N_2O might be derived from the N_2O_3 complex (1877 and 1580 cm^{-1}), which could be explained by following scheme:

$$Ce^{IV}(N_2O_3) + NO \rightarrow Ce^{IV}(NO_3) + N_2O$$

The evacuation of sample at room temperature led to an overall decrease of the absorptions due to less stable N_2O species with the eruption of a tiny peak at 2160 cm^{-1} assigned to NO^+ [30]. Ce^{IV} is a strong oxidant, and might well oxidize NO to NO^+ as can be described below:

$$NO + Ce^{IV} \rightarrow Ce^{III}(NO)^+$$

NO^+ would be present as nitrite ion, which is known to act as NO^+ donor in nitrosition [31]. Another source of NO^+ is the ionization of N_2O_3 into NO^+ and NO_2^-. However, the N_2O_3

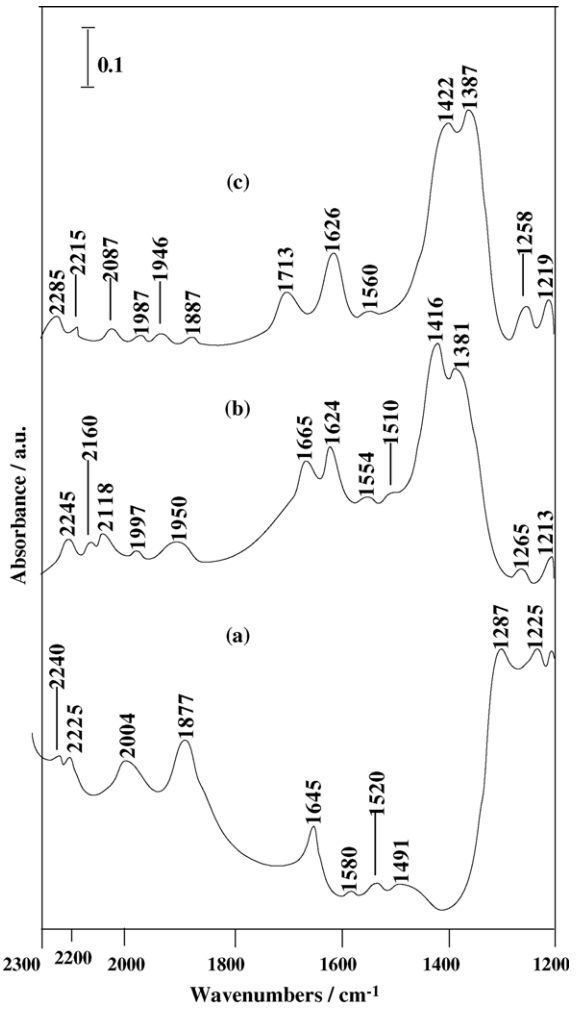

Fig. 6. FT-IR spectra of NO adsorbed on dehydrated Ce-ZSM-5_{in}: (a) in the presence of NO gas phase (50 Torr), (b) after (a) evacuation at room temperature and (c) evacuation at 50° following NO (50 Torr) adsorption at room temperature.

band at 1877(1580) cm^{-1} is much decreased in intensity (Fig. 6b), in favor of an intense doublet at 1416 and 1381 cm^{-1}, indicative of *nitrito* (oxygen-coordinated nitrite ion: ONO^-) species [32]. Simultaneously, a small hump due to NO^+ at 2160 cm^{-1} appeared. The 1645 cm^{-1} band (Fig. 6a) was developed as two bands at 1665 and 1624 cm^{-1} (Fig. 6b), which could be due to NO_2 attached to Ce in different coordination sites. The absorptions by nitrate or/and nitrite ions in general, will be referred to as NO_x^- ($x = 2$ or/and 3). The NO_x^- ($x = 2$ or/and 3) species most probably is attached to cerium cations as a result of absence of these bands on the cerium-free ZSM-5 sample.

Raising the evacuation temperature to 50 °C did not lead to significant spectral changes except the Ce^{4+}-N_2O bands was shifted from 2245 to 2285 cm^{-1} (Fig. 6c) and small spectral features related to NO (1987 and 1946 cm^{-1}) were coherently present. Besides, a new band at 1713 cm^{-1} due to Ce_{as}^{3+}-$(NO)_2$ asymmetric species was developed [33]. The doublet grew at 1422 and 1387 cm^{-1} (NO_x^-) with the band at 1626 cm^{-1} (NO_2) showed stability towards evacuation. These nitrosyl complexes may be depicted as a consequence of disproportionation of NO to NO_2 on Ce-ZSM-5_{in}. It is likely that NO_2 production at low temperatures proceeded efficiently only with the aid of redox couple (Ce^{III}/Ce^{IV}) [34]. The NO_2 production observed with Ce-ZSM-5_{in} was in line with that reported with Ce-ZSM-5 [34]. The dinitrosyl cerium complex is likely to be occurred as a result of interaction of adsorbed NO with NO in the gas phase, which subsequently converted to an unstable Ce^{IV}-N_2O and O-adsorbed species.

3.5. NO adsorption on prereduced Ce-ZSM-5_{in}

The interaction of NO on prereduced Ce-ZSM-5_{in} (500 °C, 50 Torr H_2, 1 h) is depicted in Fig. 7. The spectra showed some changes compared with those obtained from NO adsorption on dehydrated Ce-ZSM-5_{in}. Spectrum (a), taken at equilibrium with 50 Torr NO, produced bands due to NO^+ (nitrosonium ion; 2150 cm^{-1}), Ce^{4+}-N_2O (2282–2214 cm^{-1}), dinitrosyl complex species (1844, 1734 and 1720 cm^{-1}), and Ce^{4+}-NO_2 (1640 cm^{-1}). Furthermore, the appearance of maxima around 1609 and 1590 cm^{-1}, which is fully removed by short evacuation, suggests that they are due to molecularly adsorbed species, i.e. weakly bonded NO_2. The 1403, 1380 and 1360 cm^{-1} were noticed in the region of nitrato and nitrito (NO_x^-, $x = 2$–3) species [35,36]. It is worth mentioning that the bands due to N_2O_3 species were not appearing. Meanwhile the $(NO)_2$ species were predominant.

Evacuation at room temperature decreased the band intensities due to N_2O species (2245 and 2214 cm^{-1}) and Ce^{3+}-$(NO)_2$ symmetric (1869 cm^{-1}) species. The band at 1734 cm^{-1} was completely vanished with evacuation at room temperature, thereby it can be ascribed to Ce^{3+}-$(NO)_2$ at the surface. On the other hand, the absorptions owing to Ce^{4+}-NO_2 (1628 cm^{-1}) and Ce^{3+}-$(NO)_2$ asymmetric (1715 cm^{-1}) became more evident together with those for NO_x^- (1420, 1400 and 1370 cm^{-1}) species.

The NO spectra on prereduced Ce-ZSM-5_{in} taken after evacuation at 50 °C showed spectra almost similar to those observed after evacuation at room temperature. A small band at 1930 cm^{-1} due to Ce^{3+}-NO, that positioned at higher frequency than it should be (1912 cm^{-1}) is shown. This shift could be due to an induction effect from the NO_x^- species [10]. The Ce^{4+}-N_2O (2280 cm^{-1}) species was recovered (2280 cm^{-1}) at this 50 °C. This observation was associated with the persistence of NO^+ (2158 cm^{-1}) species, along with a simultaneous shifting of the band locating at 1844 cm^{-1} (spectrum a) to 1869 cm^{-1} (spectrum b) to 1877 cm^{-1} (spectrum c) with increasing evacuation temperature. Such a shift was plausibly due to gradual transformation of $(NO)_2$ to N_2O_3 species. The latter band remained strong in the spectrum of reduced Ce-ZSM-5_{in}, where it almost diminished in the spectrum of dehydrated Ce-ZSM-5_{in} sample at the same evacuation temperature. In addition, this band was

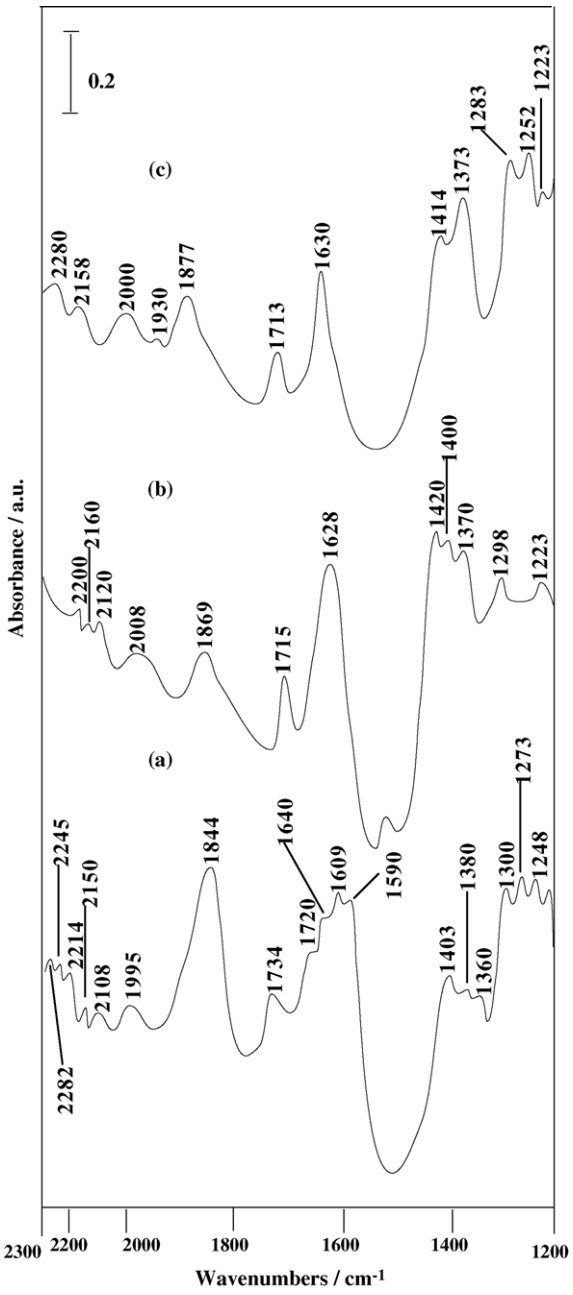

Fig. 7. FT-IR spectra of NO adsorbed on prereduced Ce-ZSM-5_{in}: (a) in the presence of NO gas phase (50 Torr), (b) after (a) evacuation at room temperature and (c) evacuation at 50° following NO (50 Torr) adsorption at room temperature.

delivered shortly after the gas admission on the dehydrated sample, dictating that N_2O_3 species is favorably adsorbed on Ce^{IV} cations. We conclude from these observations that a gradual oxidation of Ce^{III} into Ce^{IV} occurred with increasing temperature. It seems that the Ce^{3+}-cations experiencing greater electric field strength with reduction due to intervention of the cerium redox couple (Ce^{III}/Ce^{IV}). Thus, the reduction of Ce-ZSM-5_{in} with hydrogen at 500 °C brought about enhancement in the interaction–adsorption of NO.

We have observed that NO^+ (2150–2160 cm^{-1}) on prereduced Ce-ZSM-5_{in} (500 °C, 50 Torr H_2, 1 h), and this absorption band was also shown for dehydrated form of the same sample (Fig. 6). However, this species did not appear on bare ZSM-5. It suggests that the formation of NO^+ may be related to the presence of Ce cations in zeolite. NO^+ can form on the zeolite framework anion site, which becomes available due to the decreased effective charge of metal cationic species upon a coordination of NO_x^-. NO^+ and NO_x^- species are actually the ion pairs of N_2O_3 [30].

From the forgoing observations, one can conclude that the NO disproportion proceeded efficiently only with the aid of the redox couple (Ce^{III}/Ce^{IV}) as in the following scheme:

$$Ce^{III} + (NO)_2 \rightarrow Ce^{IV}(N_2O) + O^-$$

$$Ce^{IV} + NO \rightarrow Ce^{III}(NO)^+$$

$$Ce^{III}(NO)^+ + O^- \rightarrow Ce^{IV}(NO_2)^-$$

$$Ce^{III}(NO)^+ + Ce^{IV}(NO_2)^- \rightarrow Ce^{IV}(N_2O_3) + Ce^{III}$$

$$Ce^{III} + NO + 1/2O_2 \rightarrow Ce^{IV}(NO_x^-)$$

$$Ce^{IV}(NO_x^-) \rightarrow Ce^{III}(NO_2)$$

3.6. Adsorption of NO on Na-mordenite

Fig. 8 shows the spectroscopic development due to NO admission onto thermally degassed mordenite (300 °C, 3 h, 10^{-5} Torr) at room temperature in comparison with those recorded following evacuation at room temperature and at 50 °C. NO adsorption onto Na-mordenite showed bands due to N_2O (2255–2000, 1300–1220 cm^{-1}) species, NO (1894 cm^{-1}), N_2O_3 (1873 and 1610 cm^{-1}), $(NO)_2$ dimer (1860 and 1720 cm^{-1}) species, and weak bands (1680–1641 cm^{-1}) assigned to NO_2 species. The same species were also revealed on the ZSM-5 sample but showed higher intensities, comparatively.

The evacuation of sample at room temperature for 15 min almost decreased all bands except those beyond 1300 cm^{-1}. Increasing the evacuation temperature to 50 °C caused further declining of the N_2O band (2260 cm^{-1}) with almost no change in the band intensity at 1875 cm^{-1} except it accompanied a shoulder at 1890 cm^{-1}. The evacuation of sample indicated a decrease in intensities of the bands due to $(NO)_2$ as well as those of N_2O in favor of NO_2; 1636 cm^{-1}, which markedly enhanced following warming up the temperature to 50 °C. Thus, a mechanism for NO_2 formation at the expense of N_2O and $(NO)_2$ species can be proposed: NO underwent dissociation upon adsorption obviously from the observation of N_2O species even after evacuation at 50 °C. N_2O may also be resulted from the dissociation of

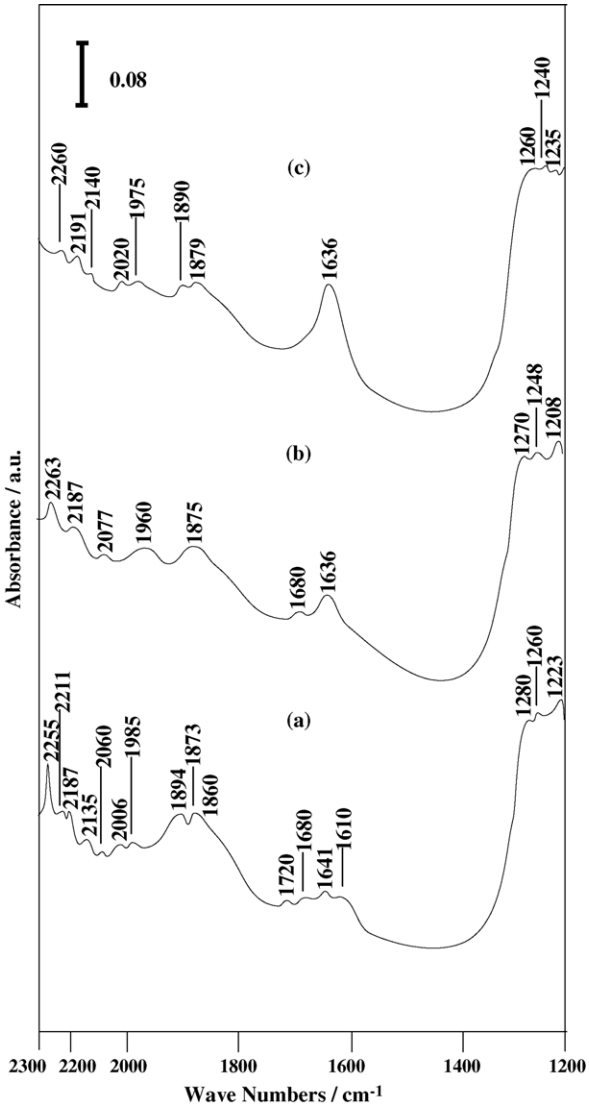

Fig. 8. FT-IR spectra of NO adsorbed on Na-mordenite, (a) in the presence of NO gas phase (50 Torr), (b) after (a) evacuation at room temperature and (c) evacuation at 50° following NO (50 Torr) adsorption at room temperature.

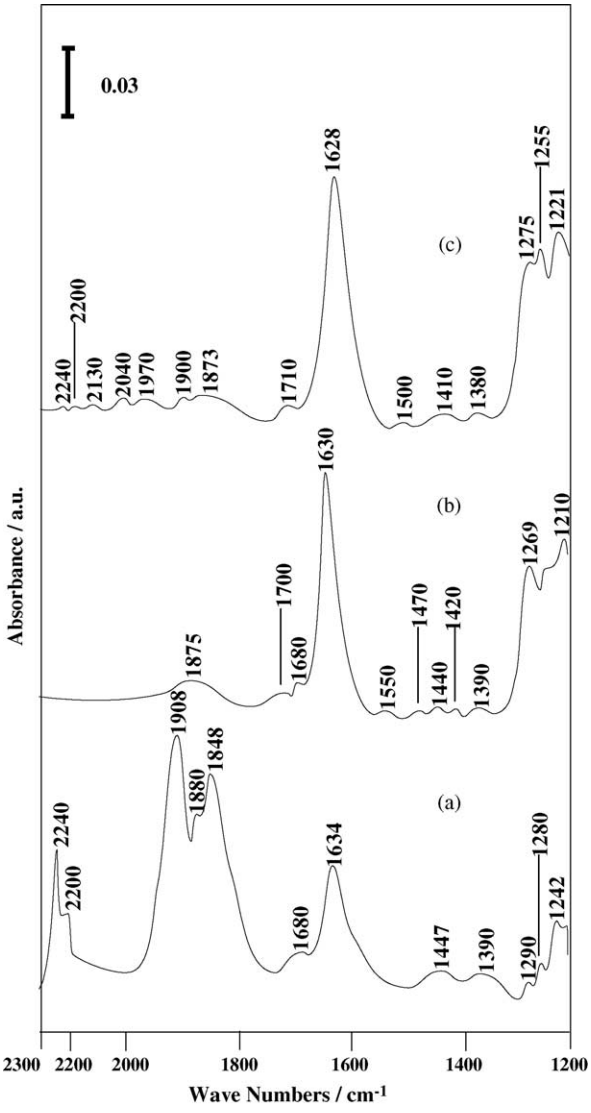

Fig. 9. FT-IR spectra of NO adsorbed on dehydrated CeM_{in}, (a) in the presence of NO gas phase (50 Torr), (b) after (a) evacuation at room temperature and (c) evacuation at 50° following NO (50 Torr) adsorption at room temperature.

$(NO)_2$ dimer adsorbed on positive charged sites; i.e. Na^+, as suggested by Cho and Lunsford [19,20]. NO_2 may be derived from dissociation of adsorbed $(NO)_2$ dimer or/and the reaction of NO with adsorbed O. The latter pathway is confirmed by the presence of visible bands at 1890 cm^{-1} due to ν(N–O) of monomeric NO species.

3.7. Adsorption of NO on Ce-mordenite

The spectrum of adsorbed NO (50 Torr equilibrium pressure) at room temperature, on dehydrated CeM_{in} sample is shown in Fig. 9, in comparison with those obtained following evacuation at room temperature and at 50 °C. Under equilibrium pressure of NO the pretreated sample showed bands of moderate intensity at 2240 and 2200 cm^{-1} due to N_2O probably adsorbed on two different surface sites [34]. A strong band at 1908 cm^{-1} due to Ce^{3+}-NO [34], together with another strong band at 1848 cm^{-1} due to Ce^{3+}-$(NO)_2$ symmetric, are detected as well. Small spectral features also appeared at 1880 cm^{-1} together with a shoulder locating around 1600 cm^{-1}, which could be obscured by the band at 1634 cm^{-1}, ascribed to N_2O_3. Other dinitrosyl small bands at 1700(1580) cm^{-1} ascribed specifically to Ce_{as}^{3+}-$(NO)_2$ are depicted in addition to the presence of a band at 1634 cm^{-1} due to Ce^{4+}-NO_2 and NO_x^- species (*nitrito* or/and *nitrato*, 1300–1500 cm^{-1}). These species were reportedly observed for NO adsorption and co-adsorption of NO and O_2 onto cerium-exchanged mordenite [30].

Evacuation of the sample at room temperature for 10 min diminished N_2O bands at 2240(2200) cm^{-1} as well as the band of Ce^{3+}-NO positioned at 1908 cm^{-1}. The

bands characterizing Ce^{3+}-$(NO)_2$ symmetric (1848 cm^{-1}) and N_2O_3 (1880 cm^{-1}), reflecting the instability of these species when they compared with the Ce^{4+}-NO_2 band (1630 cm^{-1}) which showed an enhancement in intensity. No spectral changes were depicted for *nitrito* or/and *nitrato* (1300–1500 cm^{-1}) bands and those of Ce_{as}^{3+}-$(NO)_2$ at (1700) 1680 cm^{-1}. The effect of a temperature raise to 50 °C on the different species was apparently small. However, minor variations comprised decreasing the number of bands devoted for *nitrito* or/and *nitrato* species, residual bands of NO (1900 cm^{-1}) and N_2O (2040 cm^{-1}) are developed. Of particular interest, the Ce^{4+}-NO_2 band at 1630(1628) cm^{-1} showed no changes in intensity following evacuation at 50 °C.

Comparing the IR results of dehydrated Ce-ZSM-5_{in} and CeM_{in} samples (Figs. 6 and 9), NO_x^- species is formed on Ce-ZSM-5_{in} that showed noticeable stability towards evacuation (Fig. 6). This species was reasonably derived from N_2O_3 (1877 and 1580 cm^{-1}) that ionized to NO^+ (2160 cm^{-1}) and NO_2^- (1422 cm^{-1}) (Fig. 6b). The NO_x^- ($x = 2–3$) species on Ce-ZSM-5_{in} in our oxygen-deficient conditions, is likely to be stabilized by highly coordinatively unsaturated Ce^{IV} cations in CeO_2 phase as it has been evidenced from the XRD data. The NO_x^- complexes are stable in an oxygen-rich condition, which is thought to arise from active dissociation of NO on Ce-ZSM-5_{in}. Adsorbed NO_2 on different states of Ce sites in dehydrated Ce-ZSM-5_{in}, i.e. Ce^{III}/Ce^{VI} (1665 and 1624 cm^{-1}) was devoted. It is also evident that the N_2O and $(NO)_2$ species are reversibly bound on Ce-ZSM-5_{in}. On the contrary, small spectral features of nitrosyl complexes involving, a high concentration of NO_2 species upon decomposition of NO on CeM_{in} were noticed (Fig. 9). It has been suggested previously that the redox couple (Ce^{III}/Ce^{IV}) is important in the formation of adsorbed nitrosyl species on Ce-exchanged mordenite [30]. Thus, the intervention of Ce redox couple (Ce^{III}/Ce^{IV}) was accessible in Ce-ZSM-5_{in} while inaccessible in CeM_{in}.

3.8. Adsorption of NO on prereduced cerium mordenite

The spectral changes observed upon adsorption of NO at room temperature on prereduced CeM_{in} (500 °C, 50 Torr H_2, 1 h); in comparison with those obtained following evacuation at room temperature and at 50 °C are shown in Fig. 10. At the NO adsorption pressure of 10 Torr of NO, the spectrum exhibits a spectrum similar to that of the dehydrated CeM_{in} (Fig. 9a) except, the prereduced sample offered lower concentration of NO_2 species than the latter sample. Evacuation the sample at room temperature, spectrum 10b, caused a decrease in intensity of the band characteristic of N_2O (2261 cm^{-1}). The mono-nitrosyl NO (1910 cm^{-1}) and N_2O_3 (1880 and 1610 cm^{-1}) and $(NO)_2$ symmetric (1846 cm^{-1}) bands almost diminished in favor of a marked increase in intensity of NO_2 (1636 cm^{-1}) and the NO^+ (2250 cm^{-1}) band became visible. Degassing the prereduced CeM_{in} sample at 50 °C (spectrum c) led to a

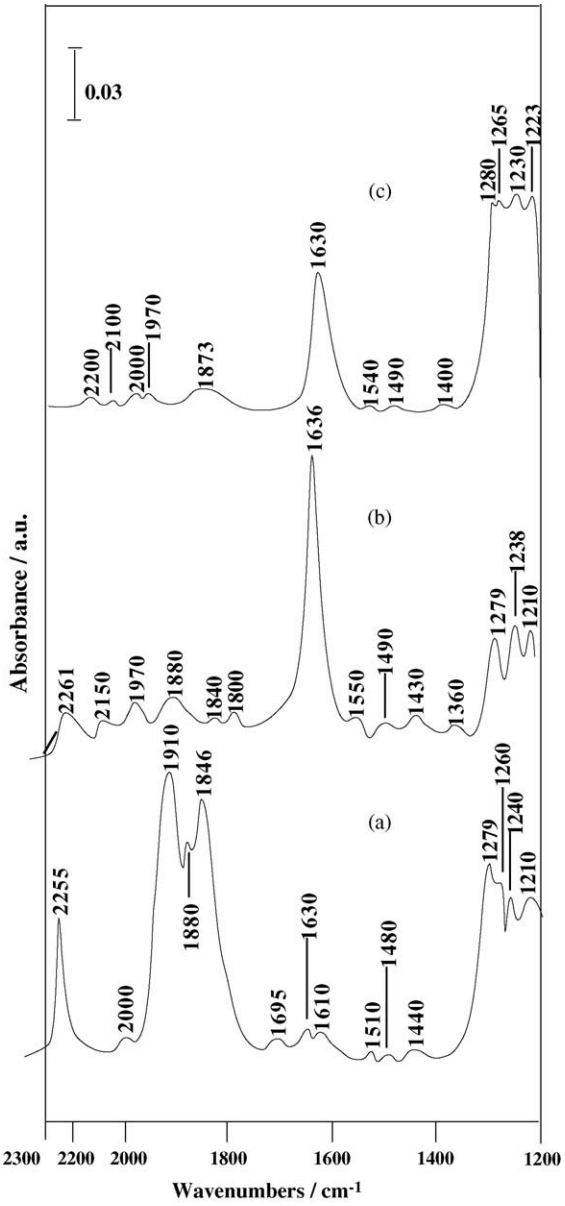

Fig. 10. FT-IR spectra of NO adsorbed on prereduced CeM_{in}, (a) in the presence of NO gas phase (50 Torr), (b) after (a) evacuation at room temperature and (c) evacuation at 50° following NO (50 Torr) adsorption at room temperature.

decrease in intensity of NO_2 (1630 cm^{-1}) band in addition to the band at 1873 cm^{-1} [$Ce^{3+}(NO)_2$]. The analysis of spectra in Figs. 9 and 10 revealed that the NO adsorption trend over dehydrated and prereduced CeM_{in} is expected to follow a similar path.

4. A comparison between Ce-ZSM-5_{in} and CeM_{in}

The results show that, prereduced Ce-ZSM-5_{in} produced bands due to appreciable amounts of nitrosyl complexes that were with lower concentrations or absent in the spectra of corresponding CeM_{in}, such as N_2O, NO^+, NO, N_2O_3, $(NO)_2$

and NO_x^-. A possible explanation for this phenomenon is related mainly to position of cerium ions in both zeolites. Undoubtedly, Ce ions embedding in the framework of zeolite as tetrahedral lattice cerium in a high symmetry environment, such as in CeM_{in}, are not electrophilic enough to form nitrosyls at ambient temperature. On the other hand, Ce^{n+} ($n = 3$–4) ions exposed to framework zeolite as octahedral Ce-oxidic moities, such as in Ce-ZSM-5_{in}, function in forming stable nitrosyl complexes. The possible explanation for the role of support on the Ce-zeolite performance in the NO adsorption–interaction is the high coordinative unsaturation of Ce-oxidic moities. Evidently, this allows easy coordination of NO_x^- anions, which proposed as intermediates in the SCR of NO_x [37].

The intervention of dual Ce^{III}/Ce^{IV} is necessary in such system, which allowed enhanced formation of absorption bands originated from NO adsorption. The inversion of Ce^{III}/Ce^{IV} is facilitated in Ce-ZSM-5_{in} but not in CeM_{in}. The production of nitrosyl complexes at lower temperatures proceeds efficiently with the aid of the redox couple Ce^{III}/Ce^{IV}. One must also consider the higher surface acidity of ZSM-5 compared with that of mordenite that can be served in enhancement of NO adsorption. However, NO possesses one more electron suited on antibonding $2\pi^*$ orbital which makes NO a slightly stronger base than CO. We indeed observed better performance of NO adsorption on unmodified ZSM-5 than on analogous mordenite (Figs. 5 and 8). These acid sites are assumed to play a role in the oxidation of NO towards NO_2 (intermediate) for NO_x reduction with NH_3, e.g. the enhanced adsorption of NH_3 [38].

5. Conclusion

Ce^{IV} framework-substituted mordenite and ZSM-5 have been hydrothermally synthesized from starting gels using *o*-phenylendiamine as a template. The XRD, FT-IR in the T–O range, unite cell parameters and textural characteristics data indicated that Ce^{IV} ions were incorporated into the framework of mordenite. On the other hand, the Ce^{IV} ions were presented in ZSM-5 as exterior cerium silicate and nano-crystallized CeO_2 phases, which associated with deformation of aluminosilicate lattice.

NO adsorption at low temperatures on the Ce^{IV}-substituted mordenite and ZSM-5 resulted in the formation of a series of nitrosyl species: N_2O (2245 cm^{-1}), NO^+ (2160 cm^{-1}), NO (1910 cm^{-1}), N_2O_3 (1880, 1580 cm^{-1}), $(NO)_{2s,as}$ (1844, 1734–1720 cm^{-1}), NO_2 (1630 cm^{-1}), and *nitrato* and *nitrito* NO_x^- ($x = 2$–3) (1300–1500 cm^{-1}).

Evacuation experiments suggest that the Ce^{n+} ($n = 3$–4) coordinated-NO_x^- anions are the most stable surface species. It has been revealed that the nitrosyl complexes were favorably formed on Ce-ZSM-5_{in} than on Ce-mordenite. The hydrogen reduction of Ce-ZSM-5 at 500 °C improved greatly its surface reactivity, and the stability of nitrosyl complexes. It has been suggested that the intervention of the cerium couple (Ce^{III}/Ce^{IV}) was facilitated on Ce-ZSM-5_{in} than on CeM_{in}. A proposed mechanism was provided for NO adsorption–interaction on prereduced Ce-ZSM-5_{in}, which seems reasonable and in particular, close homogeneous analogies to it has developed.

References

[1] S.T. Wilson, B.M. Lock, E.M. Flanigen, US Patent 4,310,440 (1982).
[2] D.B. Akolekar, J. Catal. 144 (1993) 148.
[3] E.M. Flanigen, R.L. Patton, S.T. Wilson, Stud. Surf. Sci. Catal. 37 (1988) 13.
[4] C. Kladis, S.K. Bhargava, K. Foger, D.B. Akolekar, J. Mol. Catal. A: Chem. 175 (2001) 241.
[5] M. Iwanoto, Stud. Surf. Sci. Catal. 84 (1994) 1395.
[6] K. Kaneko, A. Matsumoto, J. Phys. Chem. 93 (1989) 8090.
[7] G.B. Richter-Addo, P. Legzdins (Eds.), Metal Nitrosyl, Oxford University Press, Oxford, 1992, pp. 16–20.
[8] G. Li, K. Kaneko, S. Ozeki, Langmuer 13 (22) (1997) 5894.
[9] W.E.J. Van Kooten, B. Liang, H.C. Kijnsen, O.L. Oudshoom, H.P.A. Calis, C.M. Van der Bleek, Appl. Catal. B 21 (1999) 203.
[10] C. Kladis, S.K. Bhargava, K. Foger, D.B. Akolekara, Mol. Catal. A 175 (2001) 241.
[11] T. Komatsu, M. Nunokawa, I.S. Moon, T. Takahara, S. Namba, T. Yashima, J. Catal. 148 (1994) 427.
[12] A.V. Kucherov, C.P. Hubbard, T.N. Kucherova, M. Shelef, Appl. Catal. B 10 (1996) 285.
[13] M.M. Mokhtar, T.M. Salama, I. Othman A, G.A. El-Shobaky, Appl. Catal. A: Gen. 270 (2005) 23;
I. Othman A., Ph.D. Thesis, Faculty of Science, Chemistry Department, Al-Azhar University, Nasser City, Cairo, Egypt, 2004.
[14] A.Z.N. Christensen, Kristallography 7 (1994) 209.
[15] M. Lezcano, A. Ribotta, E. Miro, E. Lombardo, J. Petunchi, C. Moreaux, J.M. Dereppe, J. Catal. 168 (1997) 511.
[16] F. Goovaerts, E.F. Vansant, P. De Huistens, J. Gelan, J. Chem. Soc., Faraday Trans. 1 85 (11) (1989) 687.
[17] M. Yoshinobu, Kawai, Chem. Lett. (1995) 605.
[18] D.K. Paul, B.W. Smith, C.D. Marten, J. Burchett, J. Mol. Catal. A 167 (2001) 67.
[19] C.C. Cho, J.H. Lunsford, J. Am. Chem. Soc. 93 (1971) 71.
[20] C.C. Cho, J.H. Lunsford, J. Am. Chem. Soc. 93 (1971) 25.
[21] J. Valyon, W.K. Hall, J. Phys. Chem. 97 (1993) 1204.
[22] T. Cheung, S.K. Bhargava, M. Hobay, K. Foger, J. Catal. 158 (1996) 301.
[23] C. Kladis, S.K. Bhargava, K. Foger, D.B. Akolekal, J. Mol. Catal. A: 171 (2001) 243.
[24] M. Kantcheva, Appl. Catal. B 37 (2002) 1.
[25] S.H. Huang, A.B. Walters, M.A. Vannice, J. Catal. 192 (2000) 29.
[26] G. Spoto, S. Bordiga, D. Scarano, A. Zecchina, Catal. Lett. 13 (1992) 39.
[27] T.M. Salama, T. Shido, R. Onishi, M. Ichikawa, J. Chem. Soc. Chem. Comnmn. (1994) 2749.
[28] W.J. Mortier, R.A. Schoonheydt, Prog. Solid State Chem. 16 (1985) 1.
[29] M. Niwa, Y. Furukawa, Y. Murakami, J. Colloid Interf. Sci. 86 (1982) 260.
[30] E. Ito, Y.J. Mergler, B.E. Nieuwenhuys, H. van Bekkum, C.M. van den Bleek, Micropor. Mater. 4 (1995) 455.
[31] D.L.H. Williams (Ed.), Nitrosation, Cambridge Umversity Press, Cambridge, 1988.

[32] K. Nakamoto (Ed.), Infrared Spectra of Inorganic and Coordination Compounds, Wiley, New York, 1963, p. 141.
[33] A.A. Davydov, Infrared Spectroscopy of Adsorbed Species on the Surface of Transition Metal Oxides, Wiley, 1990 p. 54.
[34] S. Yokoyama, H. Yasuda, M. Misono, Shokubai 35 (1993) 122.
[35] F. Vratny, Appl. Spectrosc. 13 (1959) 59.
[36] R.E. Hester, R.A. Plane, Inorg. Chem. 3 (1964) 769.
[37] T. Tabata, H. Ohtsuka, M. Kokitsu, O. Okada, Bull. Chem. Soc. Jpn. 68 (1995) 1905.
[38] P.M. Hirsch, Environ. Prog. 1 (1982) 24.